Supporting Information

Self-assembly of magnetic DNA hydrogel as a new biomaterial for enzyme encapsulation with enhanced activity and stability

Jiayi Song, Wenting He, Hao Shen, Zixin Zhou, Mengqi Li, Ping Su* and Yi Yang*

Beijing Key Laboratory of Environmentally Harmful Chemical Analysis, College of Science, Beijing University of Chemical Technology, Beijing 100029, P.R. China.

*Corresponding authors.

Email: yangyi@mail.buct.edu.cn；suping@mail.buct.edu.cn

Tel: +86-10-64441521

1. Experiment section

1.1 Materials and instruments.

Glucose oxidase (GOx, Aspergillus niger), horseradish peroxidase (HRP), streptavidin, D-glucose, xylose, fructose, maltose, galactose, lactose, mannose, bovine serum albumin (BSA), DNase I, and 2,2′-azino-bis(3-ethylbenzothiazoline-6-sulponic acid)-diammonium salt (ABTS) were obtained from Sigma-Aldrich (USA). Fluorescein isothiocyanate (FITC) and rhodamine B isothiocyanate (RhB) were obtained from Aladdin Company (Shanghai, China). Human serum was obtained from Beijing Hospital (Beijing, China). DNA oligonucleotides were purchased and purified by Sangon Biotechnology Co. Ltd. (Shanghai, China) (Table S1).

Scanning electron microscopy (SEM, Hitachi S-4800, Japan) was used to observe the size and morphology of the prepared DNA hydrogel. The samples were directly deposited on silicon wafer, natural air dried and coated with Au and then observed by SEM. X-ray diffraction (XRD) was carried out on Rigaku Ultima diffractometer (Japan). Thermogravimetric analysis (TGA) was conducted with Mettler Toledo thermal analyzer (1100SF, USA) with an air atmosphere and a heating rate 10°C min^{-1}. The zeta potential measurement and particle size distribution were carried out in deionized water at 25°C by Zetasizer Nano-ZS (Malvern, England). The enzymatic assay were performed by UV-vis spectrophotometer (Hitachi U3010, Japan). The fluorescence measurement was confirmed by Leica confocal laser scanning microscopy (CLSM, TCS SP5II, Germany).

1.2 Preparation of biotin-functionalized DNA supramolecular chain for construction of DNA hydrogel and enzyme-DNA hydrogel.

Stoichiometric quantities of single-stranded DNA (ssDNA1, 3'-biotin modified) and ssDNA2 in Table S1 were dissolved in 10 mM PBS (pH 7.4, 0.1 M NaCl) to give a final concentration of 50 μM, and the mixture was heated to 95°C for 5 min and cooled at room temperature for 4 h to prepare the double-stranded DNA (dsDNA) supramolecular chain. The prepared dsDNA supramolecular chain (180 μL) was mixed with streptavidin (300 μL), and the mixture was incubated at room temperature for 24 h followed by centrifugation at 12000 rpm for 15 min to prepare the DNA hydrogel. For preparation of enzyme-DNA hydrogel, the dsDNA supramolecular chain (180 μL) was mixed with HRP solution (2 mM, 200 μL) or mixture of GOx solution (1 mM, 200 μL) and HRP solution (2 mM, 200 μL), respectively, and streptavidin (300 μL) was then added, respectively. The mixture was incubated at room temperature for 24 h followed by centrifugation at 12000 rpm for 15 min to prepare the HRP-DNA hydrogel and GOx&HRP-DNA hydrogel.

1.3 Encapsulation enzyme into magnetic DNA hydrogel.

The Fe_3O_4 magnetic nanoparticles were synthesized as described in our previous work.[1] The Fe_3O_4 magnetic nanoparticles (0.5 mg) were mixed with dsDNA supramolecular chain (180 μL), GOx solution (1 mM, 200 μL), and HRP solution (2 mM, 200 μL), and the mixture was incubated at 37°C for 30 min. Then, streptavidin (300 μL) was added, and the mixture was incubated at room temperature for 24 h. The products were separated by external magnetic field and washed by deionized water for 3 times to remove the unpackaged enzymes. The obtained products were denoted as GOx&HRP-magnetic DNA hydrogel. The molar ratio of streptavidin to biotin is 1:2 in this study and molar concentration of the biotin is the concentration of ssDNA1. The GOx&HRP-DNA hydrogel, GOx-magnetic DNA hydrogel, and HRP-magnetic DNA hydrogel were prepared

as the same procedure without magnetic nanoparticles, HRP, and GOx, respectively.

1.4 Enzymatic activity assay.

The encapsulated GOx&HRP (0.5 mg) were incubated with 1 mL of substrate solution, which containg 100 mM glucose and 0.5 mM ABTS, at 37°C for 5 min. The mixture was separated by external magnetic field and the supernatant of the reaction mixture was monitored with a UV-vis spectrometer at 415 nm. This assay was denoted as the standard enzymatic assay condition. The enzymatic activity assay of free GOx&HRP was same as GOx&HRP-magnetic DNA hydrogel with the same protein concentration.

Different mole ratios of GOx and HRP were encapsulated in the magnetic DNA hydrogel with the same encapsulation procedure of GOx&HRP-magnetic DNA hydrogel, and the enzymatic activity was evaluated under the standard enzymatic assay condition. The encapsulation efficiency of GOx&HRP-magnetic DNA hydrogel was investigated by incubating the GOx (1 mM, 200 μL) and HRP (2 mM, 200 μL) with the long DNA supramolecular chain (180 μL) and magnetic nanoparticles (0.5 mg) in the presence of streptavidin (300 μL) for 48 h at 29°C with interval every four hours. The leaching efficiency of enzyme and magnetic nanoparticles was tested by incubating the GOx&HRP-magnetic DNA hydrogel (0.5 mg) in the PBS buffer (10 mM, pH 7.4, 0.1 M NaCl) for 48 h at 29°C with interval every four hours. The leaching efficiency of enzyme and magnetic nanoparticles after cycles of separation was determined by continuous separation of GOx&HRP-magnetic DNA hydrogel (0.5 mg) in the PBS buffer (10 mM, pH 7.4, 0.1 M NaCl) by external magnetic field. The enzyme concentration of the supernatant for enzyme encapsulation and enzyme leaching test was determined and calculated by the Broadford method.

1.5 Stability and reusability assay.

The encapsulated GOx&HRP (0.5 mg) were incubated at 40 and 50°C for different times to determine the thermal stability, and the storage stability of the encapsulated GOx&HRP (0.5 mg) was investigated by measuring the enzymatic activity after storage at 4°C and room temperature. The solvent stability of the encapsulated enzymes (0.5 mg) against 1 mL of trypsin (1 mg mL^{-1}), ethanol, isopropanol (50 wt%, v/v), DNase I (5 Unit), and serum was investigated at 37°C for 2 h. The reusability of the encapsulated GOx&HRP (0.5 mg) was studied in PBS buffer (10 mM, pH 7.4) or serum by measuring the residual activity at 37°C after 5 min reaction. In the stability assay, the free GOx&HRP with same protein concentration was treated at a same manner with the encapsulated GOx&HRP, and all of the assay was evaluated under the standard enzymatic assay condition.

1.6 Glucose detection.

Varied concentrations of glucose were mixed with PBS buffer (1.0 mL, 10 mM, pH 7.4) containing 5 mg of GOx&HRP-magnetic DNA hydrogel and 3.0 mM ABTS, followed by incubation at 37°C for 10 min. For practical glucose detection in serum, varied concentrations of glucose were mixed with diluted serum containing 2 mg GOx&HRP-magnetic DNA hydrogel and 3.0 mM ABTS, followed by incubation at 37°C for 5 min. The encapsulated enzyme was removed by magnet, and the supernatant was monitored with a UV/vis spectrometer at 415 nm. The selectivity of GOx&HRP-magnetic DNA hydrogel toward glucose in PBS buffer (1.0 mL, 10 mM, pH 7.4) was investigated by detecting the absorbance at 415 nm in the presence of various interferes. The experiments were carried out by using 100 μM glucose, 1.0 mM of xylose, fructose, maltose,

galactose, lactose, mannose, or 1 mg mL^{-1} of BSA.

2. Results and discussion.

2.1 Preparation of DNA supramolecular chain as a scaffold for single- or multi-enzyme encapsulation.

The biotin modified single-stranded DNA (ssDNA1, 70 bases) and unmodified ssDNA2 (70 bases) are dislocation complementary, indicating that the first section of ssDNA1 is complementary to the second section of ssDNA2, and the second section of the former is complementary to the first section of the latter. The dislocation hybridization of ssDNA1 and ssDNA2 contributed to formation of long chain DNA concatemers, which consisted of multiple repeated ssDNA molecules. Therefore, the biotin groups can be well decorated into the long supramolecular chain. The zeta potential of each synthesis step was monitored, and the change of the zeta potential demonstrated the formation of the DNA supramolecular chain (Table S2). The agarose gel electrophoresis was used to further analyze the DNA supramolecular chain. As shown in Fig.S1, the DNA supramolecular chain (lane 3) migrated more slowly than each individual strand of ssDNA1 and ssDNA2 (lanes 1 and 2). The DNA supramolecular chain had large tails, indicating that the products comprised ladders of different lengths of linear dsDNA. These results demonstrated that the DNA supramolecular chain was formed as our design and that assembly was efficient. Nevertheless, the long supramolecular chain did not behave as a hydrogel. We initially investigated whether the DNA supramolecular chain could form the hydrogel in the presence of streptavidin. Streptavidin is a stable tetrameric protein, which exhibits excellent binding affinity to as many as four biotin molecules. After addition of the streptavidin, no gravitational flow was preserved within the top of the inverted vials (Fig.S2),

which indicated the formation of the hydrogel in the presence of streptavidin. Scanning electron microscopy (SEM) images indicated the DNA hydrogel was regular spherical with diameter of about 150-250 nm (Fig. S3a), which was in agreement with the dynamic light scattering (DLS) assay (Fig.S4). We then investigated whether the DNA hydrogel could be used to encapsulate single enzyme. The prepared DNA supramolecular chain was incubated with streptavidin in the presence of horseradish peroxidase (HRP). No gravitational flow was preserved within the top of the inverted vials (Fig. S5), also indicating the formation of the hydrogel in the presence of HRP. As shown in Fig. S3b, SEM images indicated the HRP-DNA hydrogel was similar to a sphere. The size (about 600 nm) was larger than that of pure DNA hydrogel, which was also confirmed by the DLS assay, and the surface morphology of HRP-DNA hydrogel was relatively rough than that of DNA hydrogel, which was attributed to the encapsulation of HRP. In order to further confirm the enzyme encapsulation, HRP was labeled with rhodamine B isothiocyanate (RhB), and the RhB-HRP was then encapsulated into the DNA hydrogel. Laser confocal fluorescence microscopy (CLSM) showed the red fluorescence, and the bright areas were consistent with the observed bright field image of CLSM (Fig. S3c and d). As shown in SEM and CLSM, the HRP was encapsulated in the inner of the hydrogel and surrounded by the external DNA supramolecular chain, which was well consistent with the encapsulation strategy by the streptavidin-biotin cross-linking.

We then wanted to know whether the length and AT/CG composition of the oligonucleotides have an influence on the efficiency of HRP encapsulation. Stoichiometric quantities of different ssDNA1 and ssDNA2 (Table S1) were used to prepare the dsDNA supramolecular chain. The prepared dsDNA supramolecular chain was mixed with HRP solution and streptavidin. The mixture was incubated at room temperature for 24 h to prepare the different HRP-DNA hydrogel, and the

HRP encapsulation efficiency was calculated. As shown in Fig. S6, about 20% of the HRP was encapsulated into the HRP-DNA-1 hydrogel (formed by 30 bases ssDNA1-1 and ssDNA2-1, Table S1), which was lower than that of HRP-DNA-hydrogel (formed by 70 bases ssDNA1 and ssDNA2, 55%) and HRP-DNA-2 hydrogel (formed by 100 bases ssDNA1-2 and ssDNA2-2, 50%). The biotin modified ssDNA1 and unmodified ssDNA2 are dislocation complementary, indicating that the first section (red parts, Table S1) of ssDNA1 is complementary to the second section (red parts, Table S1) of ssDNA2, and the second section of the former is complementary to the first section of the latter. The dislocation hybridization of ssDNA1 and ssDNA2 lead to formation of long chain DNA concatemers. The result indicated the short length of DNA bases (30 bases) may not effectively prepare the suitable DNA supramolecular chain for HRP encapsulation, therefore, the longer length of DNA bases was favorable. However, overlong ssDNA (100 bases) did not contribute to the higher enzyme encapsulation effectively, indicating the overlong ssDNA was not suitable for enzyme encapsulation. In addition, the HRP-DNA-3 hydrogel (formed by ssDNA1-3 and ssDNA2-3, Table S1), HRP-DNA-4 hydrogel (formed by ssDNA1-4 and ssDNA2-4, Table S1), and HRP-DNA-5 hydrogel (formed by ssDNA1-5 and ssDNA2-5, Table S1) only encapsulated 8.0%, 5.1%, and 6.3% HRP, respectively. Although these three ssDNA were dislocation complementary and the first section of ssDNA1 is complementary to the second section of ssDNA2, the first section of ssDNA1 is also complementary to the first section of ssDNA2 because of the lack of strict specificity of the base pair, which can significantly reduce the formation efficiency of the DNA supramolecular chain and lead to the lower enzyme encapsulation effectively. The result indicated that the casual AT/CG composition of the DNA base pair and the specific hybridization of the first section of ssDNA1 with the second section of ssDNA2 rather than the first section of ssDNA2 were important for the

formation of DNA supramolecular chain and the high enzyme encapsulation effectively. Therefore, in this work, we chose ssDNA1 and ssDNA2 in Table S1 for preparation of magnetic DNA hydrogel.

Recently, multienzyme systems have attracted great attention, and considerable efforts have been devoted to construct the novel multienzyme reactors. Because of the consecutive proceeding enzymatic reactions of the cascade reaction, each step can be well used in important applications, such as pharmaceuticals synthesis, diseases diagnosis, and enzymatic fuel cells.[2] The DNA hydrogel always preserves porous structure, which is a great benefit for guest molecule to pass through the DNA hydrogel to the active center of encapsulated enzyme.[3] We reasoned that the multienzyme encapsulated by DNA hydrogel could improve the cascade reaction efficiency. Therefore, we then wanted to know whether the prepared DNA hydrogel in this study was suitable for encapsulating multienzyme. GOx and HRP are the most widely studied cascade enzyme, and play significant important role in metabolism of the nature. We selected GOx and HRP as model enzymes, and the cascade enzymes were encapsulated to prepare GOx&HRP-DNA hydrogel through the same procedure as single HRP encapsulation. No gravitational flow was observed in the optical picture of GOx&HRP-DNA hydrogel (Fig. S7), indicating the formation of the multienzyme hydrogel. SEM image indicated that the morphology of GOx&HRP-DNA hydrogel (Fig.1b) was a little similar with HRP-DNA hydrogel, and the size of GOx&HRP-DNA hydrogel (about 2 μm) was a little larger than that of HRP-DNA hydrogel, presumably due to the larger scale of bienzyme than single enzyme. Furthermore, the surface morphology of GOx&HRP-DNA hydrogel was relatively rough than that of HRP-DNA hydrogel, which was attributed to the encapsulation of multienzyme. Agarose gel electrophoresis was used to determine the formation of DNA hydrogel and enzyme-

DNA hydrogel. As shown in Fig. S1, after addition of streptavidin, the DNA hydrogel (lanes 4), HRP-DNA hydrogel (lanes 5), and GOx&HRP-DNA hydrogel (lanes 6) were retained at the origin, indicating the formation of DNA hydrogel and enzyme-DNA hydrogel with a large structure. The zeta potential of the DNA supramolecular chain was -22.12 mV, which was lower than that of HRP-DNA hydrogel (-1.54 mV) and GOx&HRP-DNA hydrogel (8.36 mV) (Table S2), demonstrating the change of each steps towards formation of multienzyme DNA hydrogel. Ultraviolet-visible (UV-vis) absorption spectroscopy clearly indicated the location of Soret band of the heme protein at 403 nm for HRP-DNA hydrogel and GOx&HRP-DNA hydrogel (Fig. S8A), which was not changed compared with solution-state HRP. This indicated that HRP could preserved its basic secondary structure and its intrinsic activity.[4] The GOx and HRP being encapsulated in the hydrogel could retain more than 98% of their activities compared with free enzymes (Fig. S8B). The relatively high activities of GOx and HRP within the hydrogel make it a potential effective platform for further research. These results indicated the DNA hydrogel was successfully prepared, and single enzyme or multienzyme can be encapsulated into the DNA hydrogel to prepare the DNA enzyme hydrogel.

2.2 Stability of the encapsulation enzymes.

The stability of the immobilized enzyme is critical for practical applications, particularly under complex and extreme industrial environments. We investigated the thermal stability of GOx&HRP-magnetic DNA hydrogel through the preincubation of the enzyme at 40 and 50°C for different time in comparison with free enzymes. As presented in Fig. S13a and S13b, the GOx&HRP-magnetic DNA hydrogel exhibited excellent performance toward tolerance of high temperature and preserved more than 90% and 85% of enzymatic activity at 40°C and 50°C after 60 min, respectively, which were 1.6- and 1.8-fold higher than that of free enzymes. Furthermore, the storage stability of the

prepared encapsulated multienyzme was determined at 4°C and room temperature. As shown in Fig. S13c and S13d, the GOx&HRP-magnetic DNA hydrogel could preserve more than 87% of residual activity at 4°C for 9 days and 75% at room temperature for 12 days, whereas the free enzymes only preserved 36% and 19% of their original activities, respectively. The improved stabilities might ascribe to the dsDNA building blocks of the magnetic DNA hydrogel, which could effectively preserve the conformational stabilization of enzymes upon heating or long-term storage. We then investigated the enzymatic stability of free enzyme and encapsulated enzyme against protein digestion and organic solvents. As shown in Fig. 3a, the GOx&HRP-magnetic DNA hydrogel preserved most of their original activity after digestion by trypsin or incubation with isopropanol and ethanol, whereas, the free enzyme lost most of enzymatic activity at the same condition. The coating of the DNA hydrogel decreased the interaction of encapsulated enzyme with trypsin compared with free enzyme, which could protect the enzyme form degradation. Free enzymes are more easily denatured by polar organic solvents, which can compete with water to form hydrogen bonds with protein backbones, thereby disrupting the protein's conformation.[4] However, the hydrophilic DNA hydrogel provided a hydrophilic atmosphere, which can decreased the disruption of polar organic solvent. The tolerance of encapsulated enzyme in the DNase I and serum have been investigated to further evaluate its stability performance. As shown in Fig. S14, the GOx&HRP-magnetic DNA hydrogel and free enzymes could maintain more than 95% and 90% of enzymatic activity after incubation in serum, respectively, which indicated that the prepared encapsulated enzyme exhibited excellent stability towards serum. In addition, the GOx&HRP-magnetic DNA hydrogel still maintained more than 85% of enzymatic activity after incubation in DNase I, which was a little lower than that of free enzyme (89%). This might attributed to the reason that the DNA

hydrogel was partly decomposed by DNase I during incubation, and small amount of enzymes leached from the magnetic DNA hydrogel. However, this enzyme leaching after incubation with DNase I did not have a significant influence on the enzymatic assay, because more than 85% of enzymatic activity was maintained after 2 h incubation, and the standard enzymatic assay was only 5 min or 10 min.

2.3 Leaching efficiency of enzyme and magnetic nanoparticles from GOx&HRP-magnetic DNA hydrogel.

Formula S1:

Leaching efficiency (%) = amount of protein or magnetic nanoparticles in supernatant/amount of protein immobilized or magnetic nanoparticles encapsulated×100

As shown in Fig. 2d, the enzyme leaching after encapsulation might be ascribed to the adsorption of the partial enzyme on the magnetic DNA hydrogel. The magnetic nanoparticles leaching might be ascribed to the long-term incubation of the magnetic DNA hydrogel, and small amount of the magnetic nanoparticles got out of the encapsulated enzyme system.

As shown in Fig. S12, the leaching of the enzymes and magnetic nanoparticles might attributed to the continuous separation by external magnetic field, which can separate the magnetic nanoparticles and enzymes attached on the magnetic nanoparticles from the magnetic DNA hydrogel. Therefore, the leaching efficiency of magnetic nanoparticles was a little higher than that of enzymes. However, the low leaching efficiency of magnetic nanoparticles and enzymes after multiple separation have negligible impact on the overall separation performance and enzymatic

activity.

Table S1 Sequences of the DNA oligonucleotides used in the experiments.

Name	Sequence（from 5′ to 3′）
ssDNA1	CGTCCTACACTCCTGGCAGTCTCGTTCTAGTCTCG
(70 bases)	CGTTGCACCTCCGTCATGATCCATTCTCCACCTCG-biotin-3′
ssDNA2	CGAGACTAGAACGAGACTGCCAGGAGTGTAGGACG
(70 bases)	CGAGGTGGAGAATGGATCATGACGGAGGTGCAACG-3′
ssDNA1-1	CGTCCTACACTCCTG
(30 bases)	CGTTGCACCTCCGTC-biotin-3′
ssDNA2-1	CAGGAGTGTAGGACG
(30 bases)	GACGGAGGTGCAACG-3′
ssDNA1-2	CGTCCTACACTCCTGGCAGTCTCGTTCTAGTCTCGCTCGTTCTAGTCTCG
(100bases)	CGTTGCACCTCCGTCATGATCCATTCTCCACCTCGCCATTCTCCACCTCG-biotin-3′
ssDNA2-2	CGAGACTAGAACGAGCGAGACTAGAACGAGACTGCCAGGAGTGTAGGACG
(100bases)	CGAGGTGGAGAATGGCGAGGTGGAGAATGGATCATGACGGAGGTGCAACG-3′
ssDNA1-3	AAAAAAAAAATCCTGGCAGTCTCGTAAAAAAAAAA
(70bases)	CGTTGCACCTAAAAAAAAAACCATTCTCCACCTCG-biotin-3′
ssDNA2-3	TTTTTTTTTTACGAGACTGCCAGGATTTTTTTTTT
(70bases)	CGAGGTGGAGAATGGTTTTTTTTTTAGGTGCAACG-3′
ssDNA1-4	ATATATATATATATATATATATATATATATATATA
(70bases)	ATATATATATATATATATATATATATATATATATA-biotin-3′
ssDNA2-4	TATATATATATATATATATATATATATATATATAT
(70bases)	TATATATATATATATATATATATATATATATATAT-3′
ssDNA1-5	CGCGCGCGCGCGCGCGCGCGCGCGCGCGCGCGC
(70bases)	ATATATATATATATATATATATATATATATATATA-biotin-3′
ssDNA2-5	GCGCGCGCGCGCGCGCGCGCGCGCGCGCGCGCG
(70bases)	TATATATATATATATATATATATATATATATATAT-3′

The RED section of the ssDNA 1 is complementary to the RED section of the ssDNA 2; The GREEN section of the ssDNA 1 is complementary to the GREEN section of the ssDNA 2.

Table S2 Zeta potential assay after ench step for preparation of enzyme-DNA hydrogel.

Name	Zeta potential (mV)
ssDNA1	-8.56±1.34
ssDNA2	-10±1.68
DNAsupramolecular chain	-22.12±3.45
HRP-DNA hydrogel	-1.54±2.15
GOx&HRP-DNA hydrogel	8.36±1.24

Table S3 Elemental analysis of N, C, and H for Fe_3O_4 and GOx&HRP-magnetic DNA hydrogel.

	N [%]	C [%]	H [%]
Fe_3O_4	0.14	2.04	0.15
GOx&HRP-magnetic DNA hydrogel	1.83	2.85	1.53

Table S4 Kinetic parameters of GOx in free GOx&HRP and GOx&HRP-magnetic DNA hydrogel (n=3).

	K_m (mM)	V_{max} (μmol·L^{-1}·s^{-1})	k_{cat} (s^{-1})	k_{cat}/K_m (s^{-1} mM^{-1})
Free GOx&HRP	55.7	1.85	16.65	0.30
GOx&HRP-magnetic DNA hydrogel	9.4	6.29	56.61	6.02

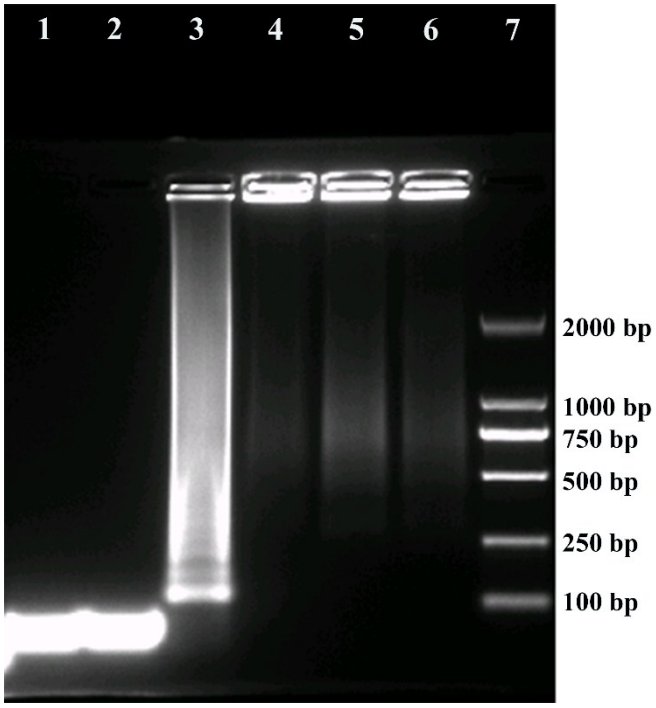

Fig. S1 Agarose gel electrophoresis: lane 1, ssDNA1; lane 2, ssDNA2; lane 3, DNA supramolecular chain; lane 4, DNA hydrogel; lane 5, HRP-DNA hydrogel; lane 6, GOx&HRP-DNA hydrogel; lane 7, biomarker.

Fig. S2 The optical image of DNA hydrogel.

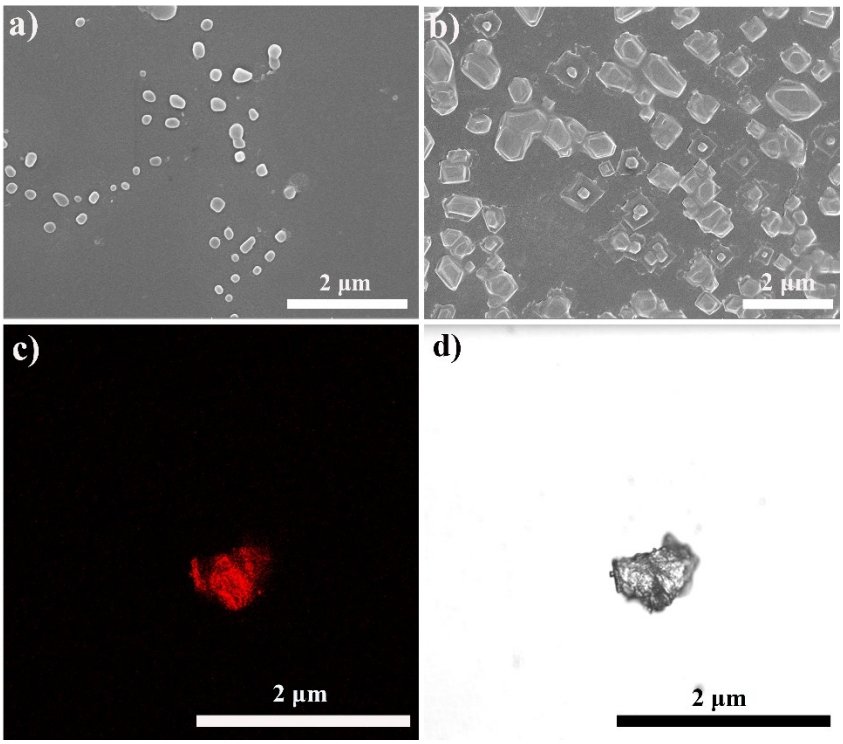

Fig.S3 SEM images of (a) DNA hydrogel and (b) HRP-DNA hydrogel; CLSM images of (c) FITC-labeled HRP-DNA hydrogel and (d) bright field image of FITC-labeled HRP-DNA hydrogel.

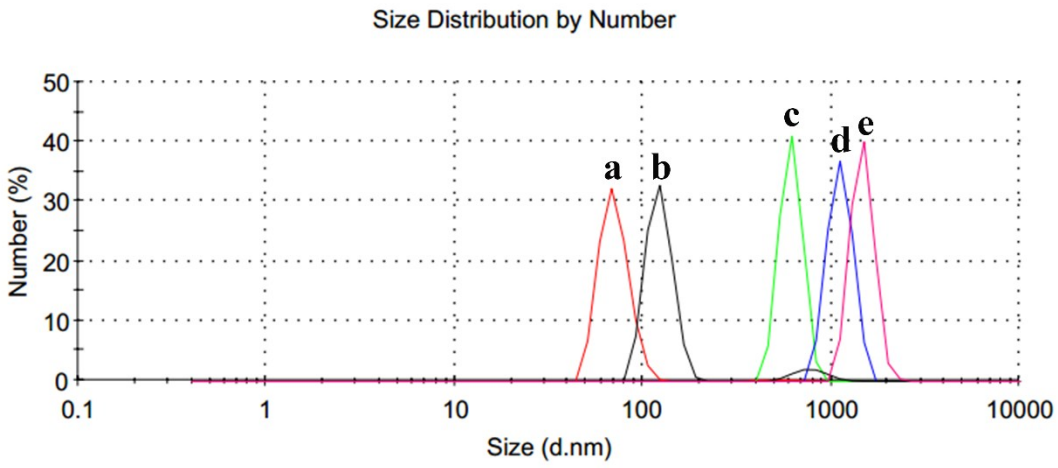

Fig. S4 Dynamic light scattering (DLS) of (a) Fe_3O_4 magnetic nanoparticles, (b) DNA hydrogel, (c) HRP-DNA hydrogel, (d) GOx&HRP-DNA hydrogel, and (e) GOx&HRP-magnetic DNA hydrogel.

Fig. S5 The optical image of HRP-DNA hydrogel.

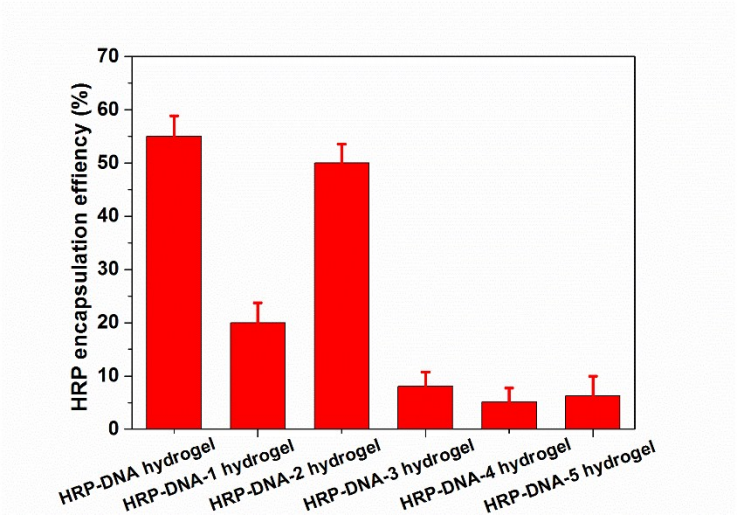

Fig. S6 Enzyme encapsulation efficiency of different length and AT/CG composition of the oligonucleotides (Table S1). The HRP-DNA hydrogel was formed by ssDNA1 and ssDNA2 (Table S1), and the HRP-DNA-1 hydrogel was formed by ssDNA1-1 and ssDNA2-1 (Table S1), and so on.

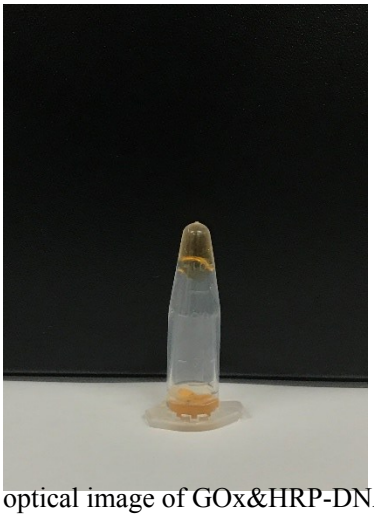

Fig. S7 The optical image of GOx&HRP-DNA hydrogel.

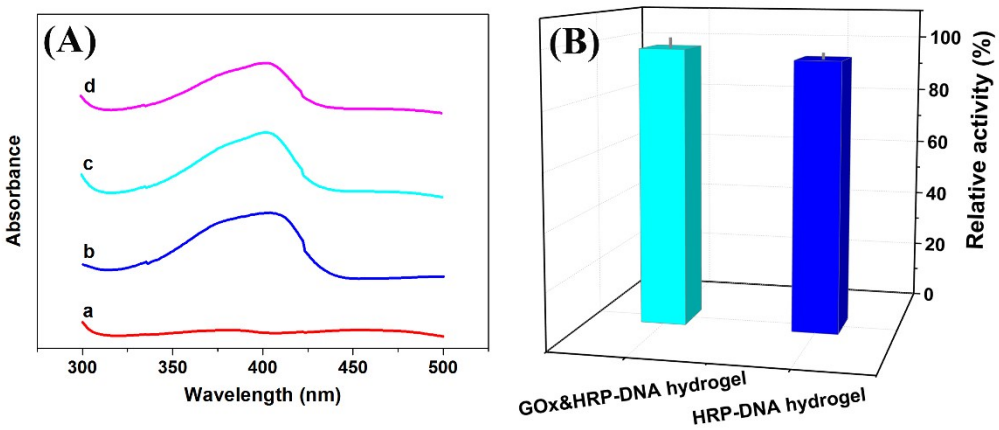

Fig. S8 (A) UV-vis spectra of DNA hydrogel (a), solution-state HRP (b), HRP-DNA hydrogel (c) and GOx&HRP-DNA hydrogel (d); (B) enzymatic activities of HRP-DNA hydrogel and GOx&HRP-DNA hydrogel compared with free HRP and GOx&HRP, respectively.

Fig. S9 The optical image of GOx&HRP-magnetic DNA hydrogel.

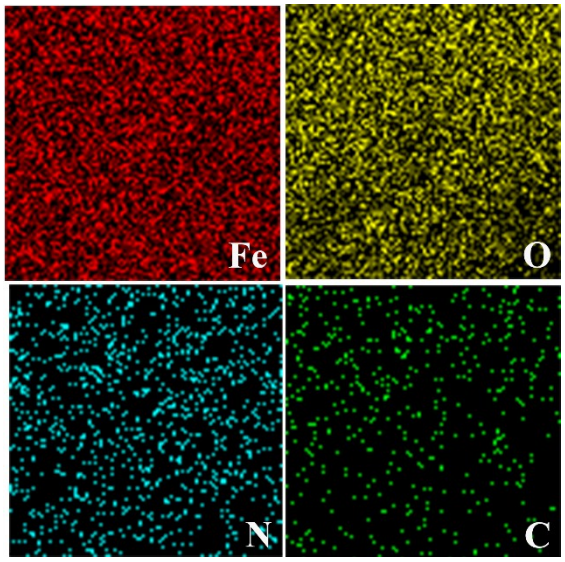

Fig. S10 EDX elemental mapping of Fe, O, C, and N of GOx&HRP-magnetic DNA hydrogel.

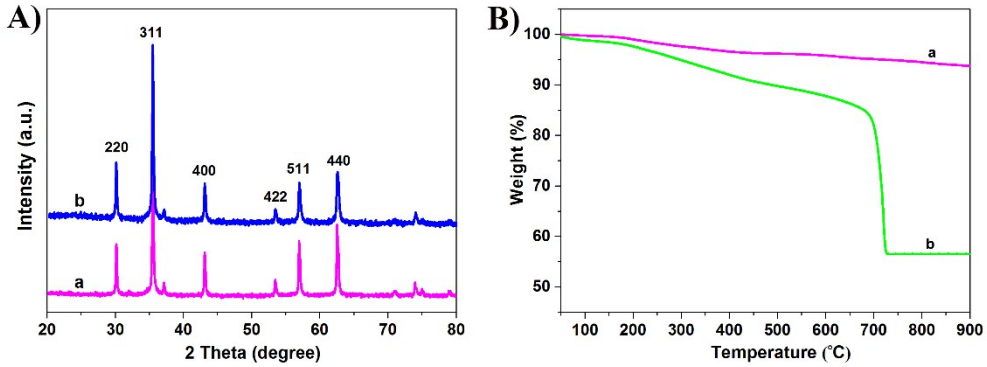

Fig. S11 (A) XRD and (B) TGA images of (a) Fe_3O_4 and (b) GOx&HRP-magnetic DNA hydrogel.

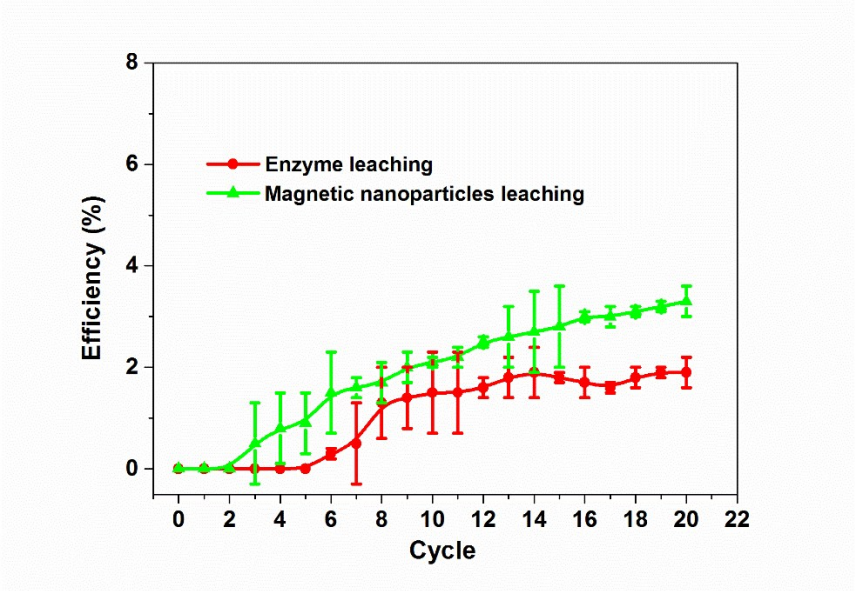

Fig. S12 The leaching efficiency of enzymes and magnetic nanoparticles after continuous separation by external magnetic field.

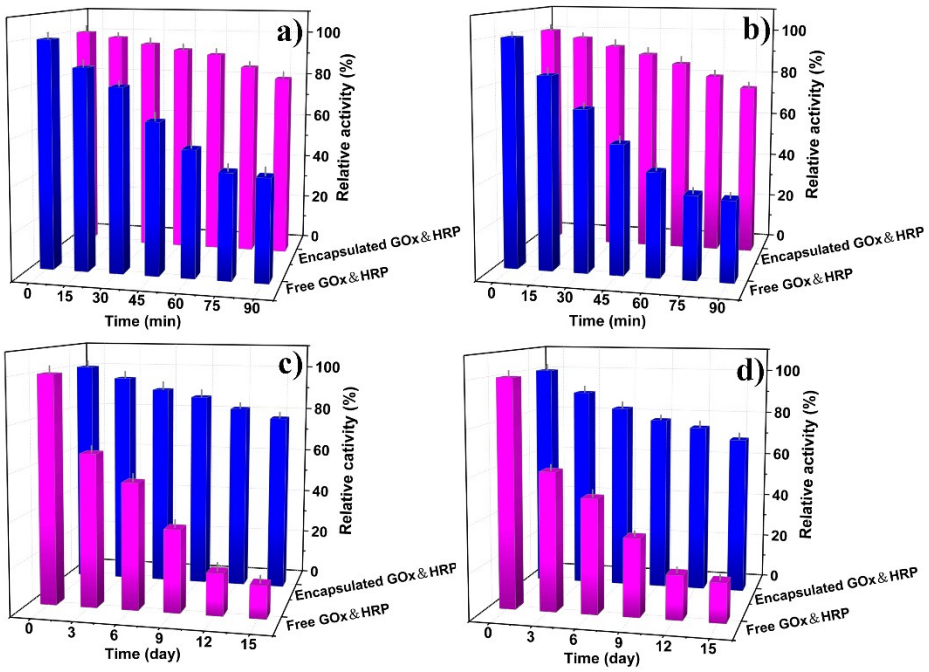

Fig. S13 (a) Stabilities of GOx&HRP-magnetic DNA hydrogel compared with free GOx&HRP: (a) thermal stability at 40°C, (b) thermal stability at 50°C, (c) storage stability at 4°C, (b) storage stability at room temperature.

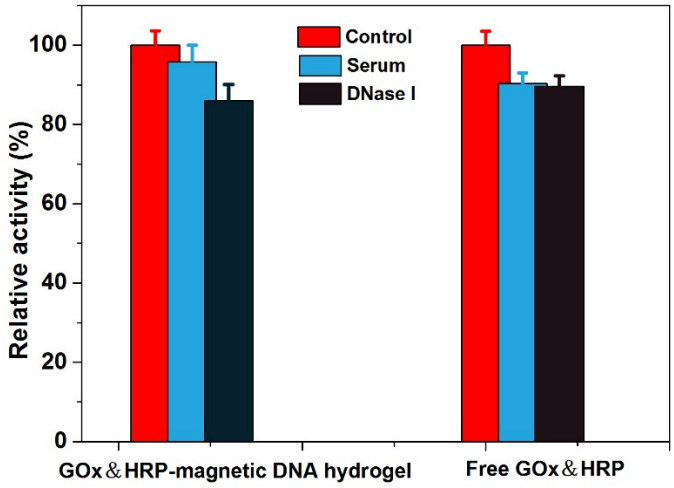

Fig. S14 Stability of GOx&HRP-magnetic DNA hydrogel and free GOx&HRP toward serum and DNase I.

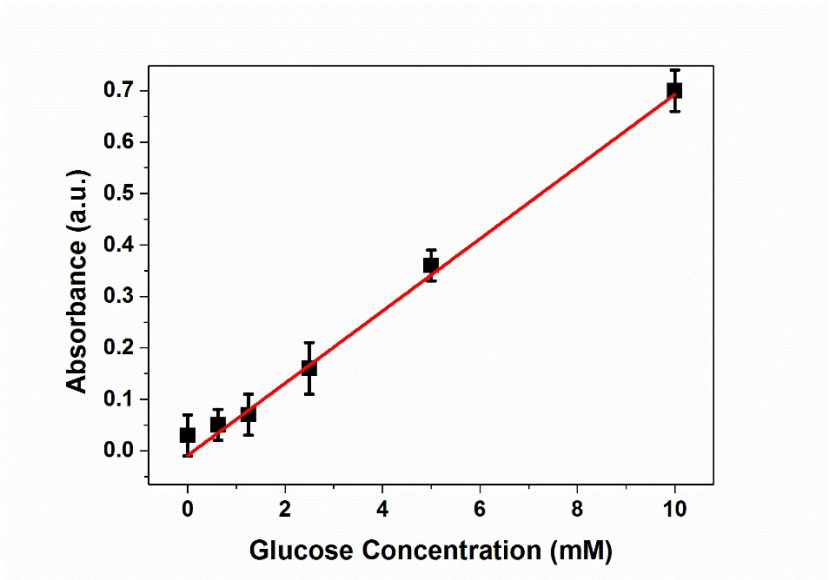

Fig. S15 Glucose detection of encapsulated enzymes with glucose concentrations of 0.625-10 mM in serum.

References

1. Y. Yang, R. Zhang, B. Zhou, J. Song, P. Su and Y. Yang, ACS Appl. Mater. Interfaces, 2017, 9, 37254.
2. (a) M. Liu, J. Fu, C. Hejesen, Y. Yang, N. W. Woodbury, K. Gothelf, Y. Liu and H. Yan, Nat.

Commun., 2013, 4, 2127; (b) S. Xu and S. D. Minteer, ACS Catal., 2013, 3, 1756; (c) D. P. Hickey, F. Giroud, D. W. Schmidtke, D. T. Glatzhofer and S. D. Minteer, ACS Catal., 2013, 3, 2729.

3. L. Wan, Q. Chen, J. Liu, X. Yang, J. Huang, L. Li, X. Guo, J. Zhang and K. Wang, Biomacromolecules, 2016, 17, 1543.
4. Q. Xie, Y. Zhao, X. Chen, H. Liu, D. G. Evans and W. Yang, Biomaterials, 2011, 32, 6588.